GEOPHYSICAL RESEARCH LETTERS, VOL. 20, NO. 12, PAGES 1135-1138, JUNE 18, 1993

AN ANOMALY IN THE AMPLITUDE RATIO OF SKKS/SKS IN THE RANGE 100–108° FROM PORTABLE TELESEISMIC DATA

Paul G. Silver
Department of Terrestrial Magnetism, Carnegie Institution of Washington

Craig Bina
Department of Geological Sciences, Northwestern University

Abstract. We have examined the amplitude ratio $SKKS/SKS$ from two deep focus events recorded by the APT89 portable seismic experiment. For one of the events (beneath the Solomon Islands), we obtain a profile of 18 stations in the distance range 99–108°. We observe large systematic variations in this ratio as a function of distance. From 99° to 106° the ratio is fairly constant and in the range 0.1 to 0.5, but it then rapidly increases to the range 0.5–3.5 between 106° and 108°. Such variations are in fact predicted by standard earth models, such as PREM, although this feature of the wavefield has not previously been observed. It is due to the momentary drop in SKS amplitude at the ray parameter where the reflected phase ScP is critically reflected. Because ray theory is not valid in this distance range, we use Full Wave theory to model the amplitudes. We have been able to match the distance pattern reasonably well if we use a model with the P-velocity at the base of the mantle reduced by 1.5% compared to PREM. Although fewer stations are available, the second event shows the same basic distance pattern, except that the abrupt increase in the ratio occurs at a closer distance. This suggests an even lower P-velocity for this region (about 3.5% slower than PREM) and is consistent with lateral heterogeneity at the base of the mantle of a few percent.

Introduction

A portable teleseismic experiment was conducted over a four month period (15 June – 15 October 1989) along a 1500km traverse in North America (see Silver et al, 1993). 22 portable three-component seismic systems were deployed: 8 instruments in a N-S line in western Ontario with approximately 50km spacing and the remaining 14 along a NE-SW line from the US-Canadian border to Wyoming with 100km spacing. The array passed through the RSON (Red Lake, Ontario) and RSSD (Black Hills South Dakota) stations, which were recording continuously (long and intermediate period channels) during the experiment. 12 of the instruments were equipped with University of Wisconsin data loggers and 3-component HS 1Hz seismometers. They triggered on P and then recorded for 20 minutes (at 25s/s) in order to assure the recording of the main S phases. 10 instruments had IRIS/PASSCAL Reftek data loggers with intermediate-period seismometers (Kinemetrics 5s and Guralp CMG3) and recorded continuously at 10s/s. Of the large suite of teleseismic events recorded, 5 possessed well-recorded SKS and $SKKS$ phases. One event in particular, 89233 (Table 1), produced excellent recordings of both of these phases at 18 of the stations. (Seismograms are shown in Silver et al. 1993.) It is this suite of recordings that constitutes the primary data set for this report. It spans the distance range 99-108°, over which the amplitude ratio of these two phases exhibits striking variations as a function of distance. As we will show, this is due to a previously unobserved phenomenon that may provide important information about the structure of the earth near the core-mantle boundary (CMB).

Data and Method

For each record, we have computed the spectral amplitude ratio $R(\omega)$ defined by

$$R(\omega) \equiv |SKKS_R(\omega)|/|SKS_R(\omega)| \qquad (1)$$

where $SKKS(\omega)$ and $SKS(\omega)$ represent the Fourier-transformed radial component of the wavelet functions for $SKKS$ and SKS, respectively. Individually, $SKKS_R(\omega)$ and $SKS_R(\omega)$, depend on several functions of frequency such as the instrument response, attenuation, and the source time function. In addition, shear wave splitting which has been observed for the stations used in this study (Silver and Kaneshima, 1993) will have a frequency dependent effect on the waveform (see Silver and Chan, 1991). Because SKS and $SKKS$ traverse nearly the same path through the mantle, each of these frequency dependent effects should cancel out of a spectral ratio. Figure 1 shows a plot of the observed ratio $R_o(\omega)$ at 0.2, 0.4, and 0.6Hz (where the signal-to-noise ratio is greatest for the largest number of stations) .

Note that at all three frequencies, $R_o(\omega)$ is fairly constant and generally in the range 0.1 to 0.5 from 100° to 106°. However, it then increases to as high as 3.5 the range 106° to 108°.

To our knowledge, this feature of wavefield has not been previously observed. Nevertheless, it is an expected feature. The ray theoretical values of $R(\omega)$ for PREM (Dziewonski and Anderson, 1981) exhibit this same behavior, except that the rapid rise occurs between 105° and 106°. The cause of this variation can be understood by considering the scattering matrix for a shear wave impinging upon the CMB from above. One obtains a reflected S wave (ScS), a reflected P wave (ScP), and a transmitted P wave (SKS). At a critical ray parameter p_{crit} (251s/rad in PREM), corresponding to a critical distance Δ_{crit}, the

Paper number 92GL02464
0094-8534/93/92GL-02464$03.00

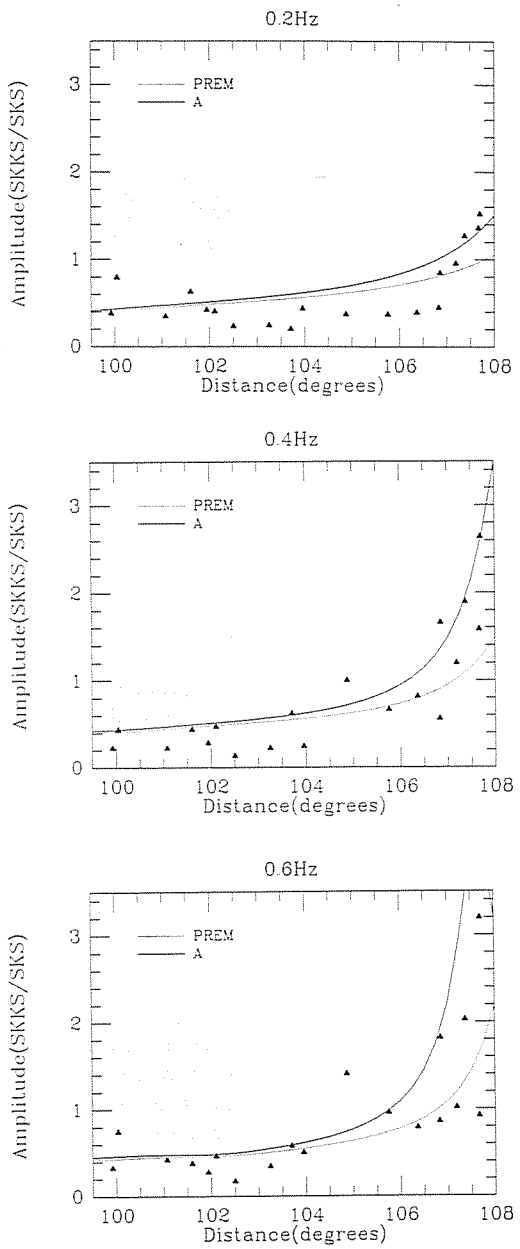

Fig. 1. Observed amplitude ratio of the radial component $SKKS/SKS$ $R_o(\omega)$ evaluated at (a) 0.2, (b) 0.4, and (c) 0.6Hz for event 89233 (see Table 1). Also shown are predicted values $R_s(\omega)$ for models PREM (dotted) and A (solid) at these same frequencies. Model A is PREM with α_{cmb} decreased 1.5%. Calculations were made using Full Wave theory.

reflected P wave attains grazing incidence: no energy is predicted to radiate into the core, and the amplitude of SKS goes to zero.

However, geometrical optics is no longer valid if the turning point of one of the phases is near a discontinuity, and a higher order theory is needed for proper interpretation. The most convenient formulation for studying this effect is Full-Wave theory (Richards, 1973, 1976), based on the Langer Approximation, which is uniformly asymptotic in approximating the radial wave functions, in particular, near a boundary. Using this formulation, Choy (1977) has shown that for finite frequencies energy does in fact radiate into the core, even at $p = p_{crit}$, in the form of the phase $SP_{diff}KS$. For distances near Δ_{crit}, this phase has nearly the same path as SKS, except that it is diffracted as a P wave for a short distance (amounting in total to $\Delta - \Delta_{crit}$) along the mantle side of the CMB, at either the source or the receiver side of the emergence point from the core or both. Thus, the profile of $R(\omega)$, particularly the location and amplitude of the peak, becomes frequency dependent as a result of the interference between SKS and $SP_{diff}KS$.

Since the location of the minimum in SKS amplitude and hence the maximum of $R(\omega)$ is controlled by p_{crit}, in principle a profile of $R(\omega) = R(\omega, p) = R(\omega, \Delta(p))$ can be used to constrain the value of p_{crit}. Because

$$p_{crit} = r_{cmb}/\alpha_{cmb}$$

this can be accomplished by varying either r_{cmb} or α_{cmb}. Since r_{cmb} is known to much greater precision than α_{cmb}, this ultimately becomes a constraint on α_{cmb}. However, we really only know $R(\omega)$ as a function of distance Δ, so that another way of fitting the data is to change the functional relationship $p = p(\Delta)$ for SKS while keeping p_{crit} fixed. For example, $p(\Delta)$ could be altered by increasing the P-velocity α_{oc} in the top several hundred km of the outer core (down to the bottoming depth of SKS) which would decrease the distance of a ray with ray parameter p_{crit}. Similarly, a shift in the integrated S-velocity of the lower mantle would also yield a change in the Δ corresponding to p_{crit}.

Comparison of the Data with Synthetics

In order to compare data with synthetics, we have calculated $R(\omega)$ for the model PREM as well as for other models with reduced α_{cmb}. In particular, we have constructed a model A simply by adopting PREM but decreasing α_{cmb} by 1.5%. The perturbation to PREM linearly changes from 0% at 150km above the CMB to -1.5% at the CMB [the properties of $SP_{diff}KS$ are apparently insensitive to the type of gradient, negative or positive (Choy, 1977)]. Synthetic amplitude ratios $R_s(\omega)$ were calculated at 0.2, 0.4 and 0.6Hz for the geometry of event 89233 (Table 1) using a Full Wave code (P. Richards, pers. comm.). Figure 1 illustrates the expected behavior both as a function of distance and of frequency. Note that the region of increase in $R_s(\omega)$ becomes more pronounced and moves to a shorter distance with increasing frequency. We note that the data share this same character. The comparison between $R_s(\omega)$ and the observed ratio $R_o(\omega)$ illustrates that PREM does not fit the data very well and that model A appears to provide a better fit.

Another way of examining the data is to compare $R_o(\omega)$ and $R_s(\omega)$ at a particular station. For this purpose, we consider station DLOR, which has exceptionally high signal-to-noise and which shows the largest amplitude anomaly. As is shown in Figure 2, the data in the 0.0–1.0Hz band show a peak value of 3.5 that is reached at about 0.5Hz. The synthetic for PREM, however, predicts that $R(\omega)$ should be a monotonically increasing function of frequency at this distance, while model A displays a function that is peaked near 0.5Hz much like the data. As with the distance dependence, this suggests a model with lower α_{cmb}.

We have examined a second event, 89215 (Table 1),

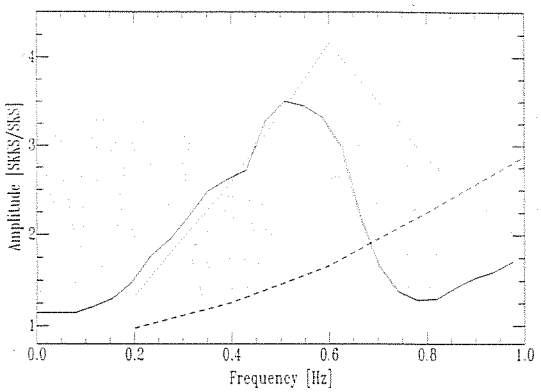

Fig. 2. For event 89233 and station DLOR, $R_o(\omega)$ (solid line) is compared to $R_s(\omega)$ for models PREM (dash) and A (dotted). Note that PREM does not fit the data very well, predicting a monotonically increasing $R_s(\omega)$ with frequency, while A predicts an $R_s(\omega)$ peak at about 0.5Hz of 3.0–4.0 as in the data.

TABLE 1. Events used

Event (yr,day)	Time, UT	Latitude (deg)	Longitude (deg)	h (km)	m_b
89233	1825:40.7	-4.09	154.45	487.1	6.0
89215	2225:57.7	-22.48	178.96	622.2	5.5

that is roughly in the same distance range. Although we have fewer data and can only reliably evaluate $R_o(\omega)$ at 0.2Hz, there is enough information to suggest the same kind of pattern as seen for 89233. In this case, however, the increase in $R_o(\omega)$ is seen at a shorter distance by about 2° (Figure 3). Only about 0.3^o can be explained by the different depths of the events (622km vs. 487km). Again, we were able to improve the fit between synthetics and data by decreasing the P-velocity of D'' (bottom 150km of the mantle). In particular, we constructed models C and E (same manner as model A) by adopting PREM but decreasing α_{cmb} by 3.3% and 4.0%, respectively.

The above analyses assume that PREM velocities are grossly correct, and the data are fit by perturbing only α_{cmb} in the model. However, as discussed above, it is also possible to fit the data by changing the functional relationship $p = p(\Delta)$ for SKS at fixed p_{crit}. For example, increasing α_{oc} by 1.7% relative to PREM yields results identical to those for model A. A uniform perturbation to the outer core velocity of this magnitude, however, would lead to large anomalies (several seconds) in the differential times $PKiKP - PcP$ which would be inconsistent with the times measured by Engdahl et al. (1974) and used to constrain the PREM outer core velocities. Thus, this sort of perturbation in the top several kilometers of the outer core would require consequent changes throughout the outer core. Alternatively, one can introduce a shift in the integrated S-velocity of the lower mantle. For example, while model PEMC (Dziewonski et al., 1975) exhibits S-velocities which average about 1.3% slower than PREM throughout the lower mantle, it yields amplitude vs. distance curves nearly identical to those obtained by adopting PREM but decreasing α_{cmb} by 1.8%. However, such large departures from PREM would be expected to result in observable travel time anomalies of several seconds.

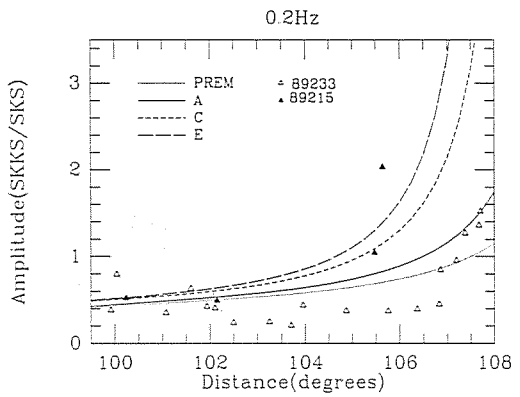

Fig. 3. Ratio $R_o(\omega)$ as a function of distance for event 89215 (solid triangles, Table 1) and 89233 (open triangles) at a frequency of 0.2Hz. Note the apparent 2° shift in the profile for 89215 relative to 89233. Also shown are predicted values $R_s(\omega)$ for models PREM (dotted), A (solid), C (short-dash), and E (long-dash) at the same frequency. Models C and E are PREM with α_{cmb} decreased 3.3% and 4.0%, respectively. Calculations were made using Full Wave theory.

Reflectivity

In order to check the systematic properties of the Full Wave synthetics, we have also generated Reflectivity seismograms (Kennett, 1983), using a code provided by T. Clarke (pers. comm.). The seismograms have been processed in the same way as the data. While thus far we have restricted our Reflectivity comparison to a frequency of 0.2Hz, we find that the general features of the distance profile, namely the location and magnitude of the peak in $R(\omega)$, are close to those obtained by the Full Wave method. We were unable to make suitable comparisons at higher frequency because the reflectivity seismograms became too noisy, presumably due to artifacts introduced by layering as noted by Choy et al. (1980). We nevertheless conclude that the two methods illustrate the same properties.

Discussion

What can we conclude about the properties near the CMB? Assuming that these observations are due to structure at the base of the mantle, they suggest that at this depth the Earth is slower than PREM in the regions sampled. More such measurements are required to determine if this is a systematic feature of the base of the mantle. Furthermore, the differences between the profiles for the two events suggest that there is lateral heterogeneity. Assuming, again, that it is on the mantle side, lateral variations of 2.0–2.5% in α_{cmb} are suggested. In principle there are two regions along the path, the source and receiver interaction points, that could give rise to the observed lateral heterogeneity, as these regions are where the phase $SP_{diff}KS$ exists. As shown in Figure 4, however, the receiver interaction points for the two events are about 250km apart at the CMB while the source points are nearly 2000km apart. Taken at face value, these data would suggest that α_{cmb} at the source interaction point for 89215 is 2.0–2.5% slower than for 89233. Also shown in Figure 4 is the lower mantle 3-dimensional P-velocity

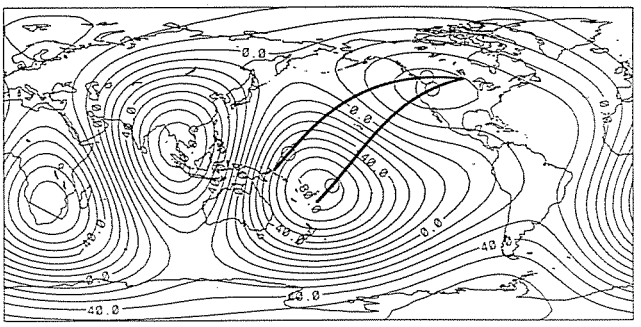

Fig. 4. World map showing event locations, event-station paths, the center of the array (station FVNR), and interaction points of SKS phases at the CMB. Also shown is the laterally varying P-velocity model L0256 (Dziewonski, 1984) evaluated at the CMB for angular orders 2 and 3 (units: m/s). Note that the interaction point for 89215 (just north of Tonga) is centered on the velocity minimum for this map, while the point for 89233 (Solomon Is.) is off to the side of this minimum. The difference in P-velocity at the base of the mantle between these two points is estimated to be 2.0–2.5% (89215 has slower velocity) based on the value of $R(\omega)$. This is in the same sense as indicated by L0256, although much greater in magnitude.

model L0256 (Dziewonski, 1984). It is evaluated at the CMB for angular orders 2-3, the part of the model for which there is agreement with other methods (Hager et al., 1985). We note that the interaction point for 89215 plots within the slowest zone in the entire map, the well-confirmed region of low velocities in the south-central Pacific. The interaction point for 89233 skirts around the side of this minimum. Thus, the difference in velocities between these two points for our data and for L0256 have the same sign, although the predicted difference for L0256, 0.25%, is an order of magnitude smaller. The variations we see, however, are consistent in magnitude with those obtained from diffraction studies in nearby areas (Wysession et al., 1992).

Acknowledgements. We especially thank Paul Richards for numerous discussions concerning the interpretation of this data set, for the use of his Full Wave code, and for a helpful review. We additionally thank Tim Clarke for discussions of the reflectivity method, Randy Kuehnel for field support and data processing, Mike Acierno for computer support, and Janice Dunlap for assistance with manuscript preparation. We acknowledge the support of the Carnegie Institution of Washington (DTM) and the National Science Foundation (EAR-9158594).

References

Choy, G., 1977. Theoretical seismograms of core phases calculated by frequency-dependent full wave theory, and their interpretation, *Geophys. J.*, *51*, 275-312.

Choy, G., V. F. Cormier, R. Kind, G. Muller, and P. G. Richards, 1980. A comparison of synthetic seismograms of core phases generated by the full wave theory and by the reflectivity method, *Geophys. J.*, *61*, 29-31.

Dziewonski, A. M., 1984. Mapping the lower mantle: Determination of lateral heterogeneity in *P* velocity up to degree and order 6, *J. Geophys. Res.*, *89*, 5929–5952.

Dziewonski, A. M., A. L. Hales, and E. R. Lapwood, 1975. Parametrically simple earth models consistent with geophysical data, *Physics Earth Planet. Int.*, *10*, 12–48.

Dziewonski, A. M. and D. L. Anderson, 1981. Preliminary reference Earth model, *Physics Earth Planet. Int.*, *25*, 297–356.

Engdahl, E. R. , E. A. Flinn, and R. P. Masse, 1974. Differential PKiKP travel times and the radius of the inner core, *Geophys. J.* *39*, 457-464.

Hager, B. H., R. W. Clayton, M. A. Richards, R. P. Comer, and A. M. Dziewonski, 1985. Lower mantle heterogeneity, dynamic topography and the geoid, *Nature*, *313*, 541–545.

Kennett, B. L. N, 1983. *Seismic Wave Propagation in Stratified Media*, Cambridge University Press, Cambridge, UK.

Richards, P. G., 1973. Calculation of body waves for caustics and tunnelling in core phases, *Geophys. J. R. astr Soc.*, *35*, 243-264.

Richards, P. G., 1976. On the adequacy of plane wave reflection/transmission coefficients in the analysis of seismic body waves, *Bull. seism. Soc. Am.*, *66*, 701-718.

Silver, P. G. and W. W. Chan, 1991. Shear-wave splitting and subcontinental mantle deformation, *J. Geophys Res.* *96*, 16,429-16,454.

Silver, P. G. and S. Kaneshima, 1993. Constraints on mantle anisotropy beneath precambrian North America from a transportable teleseismic experiment, *Geophys Res Lett*, this issue.

Silver, P. G., R. B. Meyer, and D. E. James, 1993. Intermediate-scale observations of the Earth's deep interior from the APT89 transportable teleseismic experiment, *Geophys. Res. Lett.*, this issue.

Wysession, M. E., E. A. Okal, and C. R. Bina, 1992. The structure of the core-mantle boundary from diffracted waves, *J. Geophys. Res.*, *97*, 8749–8764.

P. G. Silver, Department of Terrestrial Magnetism, Carnegie Institution of Washington, 5241 Broad Branch Road, N.W., Washington, D.C. 20015.

Craig Bina, Department of Geological Sciences, Northwestern University, 1847 Sheridan Road, Evanston, IL 60208.

(Received: August 4, 1992;
revised: September 10, 1992;
accepted: October 13, 1992.)